

Integral Curve Clustering and Simplification for Flow Visualization: A Comparative Evaluation

Lieyu Shi, Robert S. Laramee, *Member, IEEE*, and Guoning Chen, *Member, IEEE*

Abstract—This document provides supplementary materials to the submission.

Index Terms—Clustering technique, similarity measures, flow visualization, experimental study, empirical guidelines, quantitative comparisons.

1 INTRODUCTION

THIS document provides additional description on the experimental setups (Sect. 2), ground-truth verification (Sect. 3), and additional results (Sect. 4, Sect. 5, Sect. 6 and Sect. 7) for the paper submission, *Integral Curve Clustering and Simplification for Flow Visualization: A Comparative Evaluation*.

2 SIMILARITY MEASURES AND OPTIMAL CLUSTERS

In this section, we introduce a number of popular similarity measures that are implemented for our integral curve clustering. We also discuss based on these similarity measures how many optimal clusters are generated by the two methods described in the paper, i.e., the SC with eigen-rotation and the hierarchical L-method.

2.1 Similarity Measures

Given m -dimensional candidate curves \mathbf{x} and \mathbf{y} , they can have two representations, i.e., $\mathbf{x} = (\mathbf{x}^{(1)}, \mathbf{x}^{(2)}, \dots, \mathbf{x}^{(m)})$ as a coordinate representation, and $\mathbf{x} = (\mathbf{v}_x^{(1)}, \mathbf{v}_x^{(2)}, \dots, \mathbf{v}_x^{(c)})$ ($c \equiv \frac{m}{3}$) as a vertex representation.

1) Euclidean distance $d_E(\cdot, \cdot)$, with complexity of $O(m)$.

2) Fraction norm $d_F(\cdot, \cdot)$

This similarity measure is taken from Aggarwal et al. [1] and can address *curve of dimensionality* for high-dimensional space:

$$d_F(\mathbf{x}, \mathbf{y}) = \left(\sum_{i=1}^m \| \mathbf{x}^{(i)} - \mathbf{y}^{(i)} \|^p \right)^{\frac{1}{p}} \quad (1)$$

where $p < 1$. In our experiment we set $p = 0.5$. d_F has complexity of $O(m)$.

3) Geometric similarity measure $d_G(\cdot, \cdot)$

• L. Shi and G. Chen are with the Department of Computer Science, University of Houston, Houston, TX, 77004. E-mail: guoning.chen@gmail.com
 • R. S. Laramee is an Associate Professor of the Department of Computer Science, Swansea University, SA2 8PP, Wales, UK. Email: R.S.Laramee@swansea.ac.uk

Proposed by Shi and Chen [2] based on the intuition that two curves are considered similar in shape if their pair of piece-wise line segments are parallel.

$$d_G(\mathbf{x}, \mathbf{y}) = \text{mean}_{1 \leq i \leq c-1} \arccos \frac{(\mathbf{v}_x^{(i+1)} - \mathbf{v}_x^{(i)}) \cdot (\mathbf{v}_y^{(i+1)} - \mathbf{v}_y^{(i)})}{\| \mathbf{v}_x^{(i+1)} - \mathbf{v}_x^{(i)} \| \| \mathbf{v}_y^{(i+1)} - \mathbf{v}_y^{(i)} \|} \quad (2)$$

The complexity of d_G is $O(m)$.

4) Accumulated rotation difference $d_R(\cdot, \cdot)$

Accumulated rotation measures the summation of discrete curvature along the whole curve, hence d_R can be described as

$$d_R(\mathbf{x}, \mathbf{y}) = \| d_r((\mathbf{x})) - d_r(\mathbf{y}) \| \quad (3)$$

$$d_r(\mathbf{x}) = \sum_i \arccos \frac{(\mathbf{v}_x^{(i+1)} - \mathbf{v}_x^{(i)}) \cdot (\mathbf{v}_x^{(i+2)} - \mathbf{v}_x^{(i+1)})}{\| \mathbf{v}_x^{(i+1)} - \mathbf{v}_x^{(i)} \| \| \mathbf{v}_x^{(i+2)} - \mathbf{v}_x^{(i+1)} \|} \quad (4)$$

The complexity of d_R is $O(m)$.

5) Mean-of-closest-point (MCP) $d_M(\cdot, \cdot)$

$$d_M(\mathbf{x}, \mathbf{y}) = \text{mean}(d_m(\mathbf{x}, \mathbf{y}) + d_m(\mathbf{y}, \mathbf{x})) \quad (4)$$

$$d_m(\mathbf{x}, \mathbf{y}) = \text{mean}_{\mathbf{v}^{(l)} \in \mathbf{x}} \min_{\mathbf{v}^{(k)} \in \mathbf{y}} \| \mathbf{v}^{(l)} - \mathbf{v}^{(k)} \| \quad (5)$$

d_M is taken as state-of-art similarity measures for integral curves and its complexity of computing $d_M(\cdot, \cdot)$ is $O(m^2)$.

6) Hausdorff distance $d_H(\cdot, \cdot)$

$$d_H(\mathbf{x}, \mathbf{y}) = \max \{ d_h(\mathbf{x}, \mathbf{y}), d_h(\mathbf{y}, \mathbf{x}) \} \quad (6)$$

$$d_h(\mathbf{x}, \mathbf{y}) = \sup \{ d(\mathbf{s}_i, \mathbf{y}) | \mathbf{s}_i \in \mathbf{x} \}$$

$d_H(\cdot, \cdot)$ is taken from Rossl and Theisel [3] and it is topologically meaningful for building a metric space. Similar to $d_M(\cdot, \cdot)$, the complexity of computing $d_H(\cdot, \cdot)$ is $O(m^2)$.

7) Signature-based measure $d_S(\cdot, \cdot)$

This hierarchical signature-based similarity measure in Eq. 7 is taken from McLoughlin et al. [4], which uses a combination of both closest-point-distance and χ^2 test of streamline signatures. To simplify the implementation, we only consider discrete curvature as signature and preset

TABLE 1
Meta-data of tested flow data sets

	Cylinder	Bernard	Crayfish	Tornado	Solar Plume	Hurricane	Tube	Cylinder Pathlines	Blood Flow
Curve Numbers	9,207	7,086	3,737	5,468	4,799	7,451	2,015	2,590	547
Max Dimension	1,800	1,998	1,836	603	6,006	4,824	345	303	1,935

a fixed bin size for each data set. Additionally, we set $\alpha = 0.5$.

$$d_S(\mathbf{x}, \mathbf{y}) = (1 - \alpha)\chi^2(P_x, P_y) + \alpha \cdot mean_dist(\mathbf{x}, \mathbf{y}) \quad (7)$$

$$\chi^2(P_A, P_B) = \sum_{bin \in B} (P_{bin,A} - P_{bin,B})^2 / (P_{bin,A} + P_{bin,B})$$

The complexity of d_S is $O(m^2)$ due to that second half of Eq. 7 involves MCP distance on under-sampled curves.

- 8) Adapted Procrustes distance $d_P(\cdot, \cdot)$

$d_P(\cdot, \cdot)$ is taken from Tao et al. [5], [6] which is defined as Euclidean distance after Procrustes superimposition [7] (s is a scaling factor, \mathbf{E} is a rotational matrix and \mathbf{T} is the translation, respectively).

$$d_P(\mathbf{x}, \mathbf{y}) = mean_{\mathbf{v}_x^{(i)} \in \mathbf{x}, \mathbf{v}_y^{(i)} \in \mathbf{y}} d_p(\mathbf{v}_x^{(i)}, \mathbf{v}_y^{(i)}) \quad (8)$$

$$d_p(\mathbf{v}_x^{(i)}, \mathbf{v}_y^{(i)}) = \min_{s \in \mathbb{R}^+, \mathbf{E} \in \mathbb{R}^{m \times m}, \mathbf{T} \in \mathbb{R}^m} d_E^2(\mathbf{v}_x^{(i)}, \mathbf{v}_y^{(i)'})) \quad (9)$$

$$\mathbf{v}_y^{(i)'} = s\mathbf{E}\mathbf{v}_y^{(i)} + \mathbf{T}$$

where the orthogonal Procrustes estimate for \mathbf{E} relies on singular value decomposition and hence has complexity of $O(r^3)$ (r is the dimension of point set \mathbf{v}_{xi} and \mathbf{v}_{yi} , and we set it to 7 as in [5], [6]). d_P is scaling-free, translation-free and rotation-free with high cost in computation. Firstly pairwise distance between vertex \mathbf{x} and \mathbf{y} is computed as Procrustes distance between their 7 neighboring point set in Eq. 9, and the final distance is the mean of those vertex pairs in Eq. 8. The complexity is $O(m)$.

- 9) Time-series MCP $d_T(\cdot, \cdot)$, introduced in Meuschke et al. [8], [9] which is MCP considering time interval overlapping and mismatching in Eq. 10. This similarity measure is specifically designed for temporal pathline similarity computation.

$$d_T(k, l) = \frac{1}{t_M - t_1} \sum_{i=1}^{M-1} (t_{i+1} - t_i) \cdot \bar{D}^{kl}(t_i, t_{i+1}) \quad (10)$$

$$\bar{D}^{kl}(t_i, t_{i+1}) = \int_0^1 d(t) dt = \int_0^1 \sqrt{a + 2bt + ct^2} dt$$

Note that, since the pathlines used in our experiment are with consistent time steps starting from the same time and after direct filling strategy (see Sect. 3.4), any two pathlines share the same time intervals, only **Case 1** is needed in d_T computation as in [8], [9]. Besides, Jaccard matrix computation is no longer needed. The complexity is $O(m)$ if Jaccard matrix is not needed otherwise $O(m^2)$.

2.2 SC and L-method

In order to validate and compare the two optimal-cluster-number determination strategies mentioned in the paper, we firstly experiment on 8 different point cloud data sets and 2 streamline data sets as illustrated in Fig. 1 (the point cloud data sets and implementation of the two methods are released in github¹). For

point cloud clustering, we use single-linkage AHC to perform the hierarchical L-method computation, while for streamline data sets we applied Mean-of-closest-point (MCP) distance (i.e., d_M in Sect. 2) and average-linkage AHC (because average-linkage is most dominant in flow visualization). Despite being able to detect more accurate clusters than SC with eigen-rotation in cloud points (in Fig. 1(a) and 1(b)), L-method does not showcase further advantage over SC with eigen-rotation in streamline data sets (in Fig. 1(c) and 1(d)). This is due to the absence of unambiguous ground truth for the number of clusters that are naturally perceived for streamlines even for very simple streamline data sets, such as Bernard and tornado.

Without knowing which one is better for a particular data set, we utilize both SC eigen-rotation and the hierarchical L-method to determine the optimal number of clusters and the result cluster numbers are reported in Table 2. The following provides a more detailed discussion on the characteristics of the two approaches in determining the optimal cluster numbers for the testing data sets.

Hierarchical L-method

The L-method tends to determine either less than 5 clusters or very large number of clusters since it optimally searches the global knee of the “cluster-number vs. merged-distance” graph from 2 to the total number of streamlines/pathlines in the data. Besides, it works reasonably well for pretty simple data sets in spatial clustering, e.g., streamlines of the Bernard which has intrinsically 4 clusters (see Fig. 2(a) and 2(b)).

SC with eigen-rotation

SC with eigen-rotation can often detect more clusters than the hierarchical the L-method for the same similarity measure. Compared to a stable solution by the L-method, SC with eigen-rotation highly relies on k (initial input number so that ultimately optimal cluster can be found within range $[1, k]$) and suffers greatly from computational cost as k increases. Simply choosing $k = 100$ takes more than tens of hours to compute the optimal number of clusters as shown in Table 3, and if optimal number of clusters from prior-knowledge is larger, then SC with eigen-rotation will be not efficient.

3 GROUND-TRUTH VERIFICATION

We also verify our implementation on clustering algorithms and similarity measures for the Bernard streamline data set which is known by the flow visualization and application communities to have 4 clusters. The segmentation of streamlines for the Bernard data set is illustrated in Fig. 2. The number of clusters determined by the hierarchical L-method is closer to the ground-truth value, hence AHC-average with d_M and d_H are displayed. Besides, Fig. 2 shows that k-means can better capture the four anticipated streamline bundles than PCA-AHC-average, which further justifies why we apply k-means instead of AHC-average for PCA clustering as discussed in in Sect. 3.2 of the paper. We also show the average-AHC and SC-k-means with d_M and d_H for Bernard, and the SC eigen-rotation with d_M and d_H with k initialized as 10. Due to the fuzzy partitioning boundary as displayed in the simplified Bernard data (see Fig. 1(c) and Fig. 1(d)), four streamline bundles are not

1. <https://github.com/lieyushi/ClusterTestingDemo>

TABLE 2
Optimal cluster numbers with SC eigen-rotation (left) and L-method (right) for the 9 experimental data sets

	d_E	d_F	d_G	d_R	d_M	d_H	d_S	d_P	d_T
Flow behind cylinder	15 3	35 3	18 3	17 3	25 3	26 4	33 3	2 10	- -
Bernard	28 4	19 4	21 42	20 3	25 3	15 3	34 17	2 4	- -
Crayfish	20 3	20 4	22 3	13 3	37 3	29 3	28 3	24 3	- -
Tornado	24 4	16 3	16 3	11 3	11 3	16 7	18 3	13 3	- -
Hurricane	2 4	2 6	14 5107	30 4	2 4	12 3	13 3	19 728	- -
Solar Plume	33 3	24 7	21 3	17 3	10 3	3 3	2 4	2 9	- -
Cylinder Pathlines	10 3	17 5	2 1794	9 3	17 4	3 4	15 3	14 3	14 3
Tube Pathlines	15 4	9 5	14 4	15 3	15 3	17 5	15 3	15 3	12 5
Blood Flow	2 3	9 3	13 361	4 3	2 3	3 8	3 8	4 3	2 4

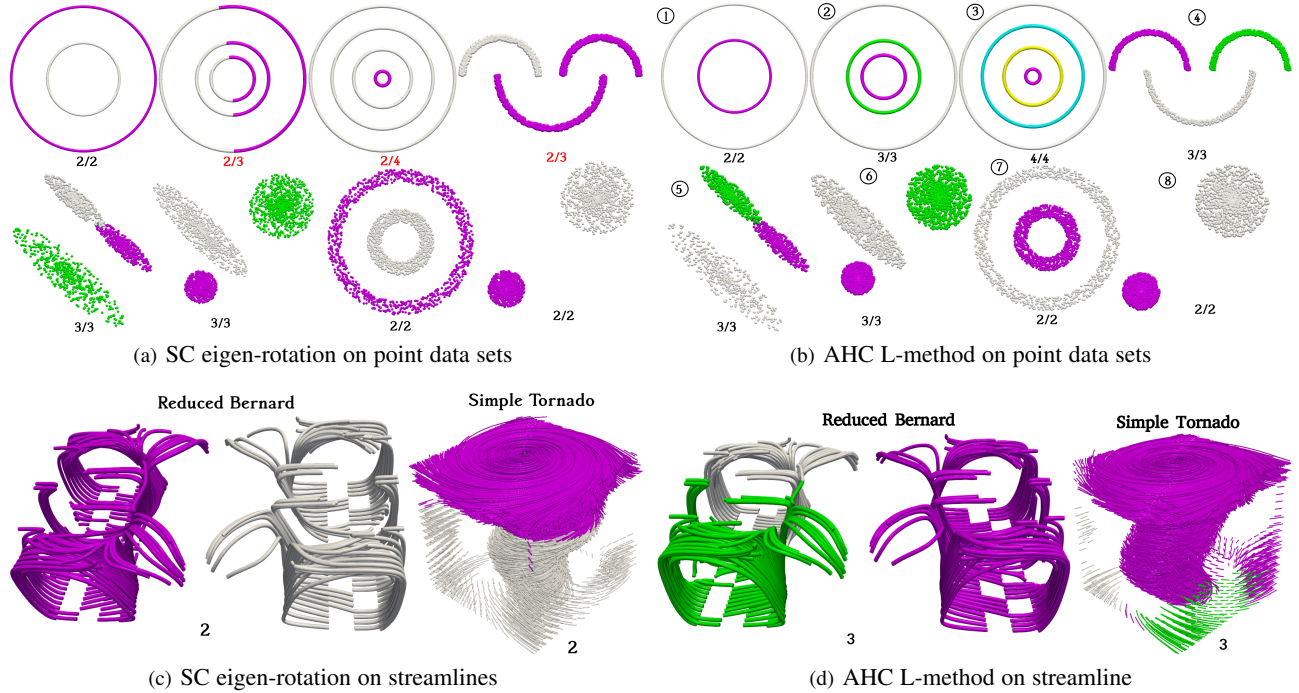


Fig. 1. Comparison of SC eigen-rotation minimization and the AHC L-method for detecting the optimal number of clusters in the tested point cloud (top row) and streamline data sets (bottom row). The number below each point cloud figure in Fig. 1(a) and Fig. 1(b) indicates detected/true cluster numbers respectively (incorrect detected cluster numbers are marked in red), and number below each figure in Fig. 1(c) and Fig. 1(d) displays the detected number of streamlines. We find that hierarchical L-method is slightly better than SC eigen-rotation in detecting optimal clusters of point cloud data sets, while for streamline data sets it is difficult to decide which one is better since there is no ground truth for how many clusters reside in streamlines.

entirely distinct by clustering algorithms, and often only 3 or 2 bundles of streamlines are distinguishable.

4 QUANTITATIVE EVALUATION RESULT

The average performance (computation time) is listed in Table 3 (streamlines) and Table 4 (pathlines). The quantitative evaluation results of clustering techniques combined with different similarity measures are displayed respectively for streamline data sets, i.e., cylinder (in Table 5), Bernard (in Table 6), crayfish (in Table 7), tornado (in Table 8), solar plume (in Table 9), and pathline data sets, i.e., cylinder pathlines (in Table 11), tube pathlines (in Table 12) and blood flow pathlines (in Table 13).

Note that, values in a cell of the tables (i.e. Tables 5, 6, 7, 8, 9, 11, 12, 16, 17 and 13) are, silhouette (top left), Hubert's Γ statistic (top right), Davies-Bouldin index (bottom left) and (normalized) validity measurement (bottom right). xxxx and xxxx denotes the maximal silhouette and Hubert's Γ statistic of each column, while xxxx* and xxxx denotes the minimal Davies-Bouldin index and validity measurement, respectively in the tables.

In addition to the two-level affinity propagation (AP) by Tao et al. [5], [6], we also implement the single-level AP (the original method of AP clustering [10]) and show the results in Table 14. Since single-level AP often generates thousands of clusters as discussed by Tao et al. [5], [6], we prefer not to discuss the single-level AP in our evaluations and using two-level AP instead in the paper (remarked for AP for short in all the contents). Nonetheless, we provide the results for the single-level AP for interested readers.

We also provide the resulted number of clusters generated by both single-level and two-level AP clustering techniques with various similarity measures on all data sets in Table 15. It clearly shows that while single-level AP usually generates too many clusters, two-level AP either produces too many or too few clusters which does not completely resolve the issues of AP in flow visualization.

5 RANKING BASED VISUALIZATION

In this section we use a ranking-based visualization technique to denote in each evaluation index which clustering algorithm and

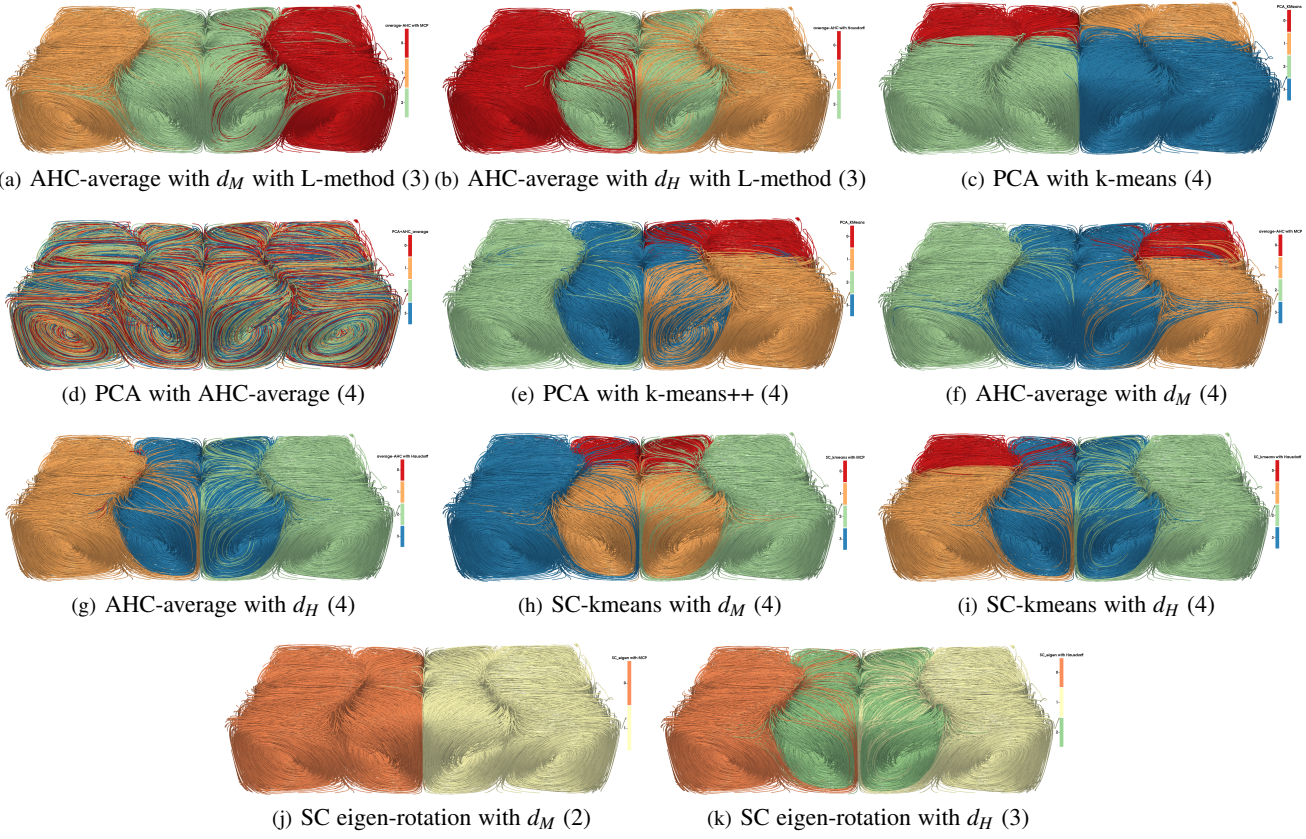


Fig. 2. Clustering verification on segmentation of bernard streamline data set with number of clusters in the parenthesis. (a)(b) are the optimal segmentation of streamlines with d_M and d_H by hierachical L-method. Since the ground-truth cluster numbers are 4, we set 4 as input for PCA, AHC-average and SC k-means with d_M and d_H , and 10 for SC eigen-rotation with d_M and d_H in Fig. 2(j) and Fig. 2(k).

TABLE 3
Average computation time (in minutes)* for clustering techniques with various similarity measures for streamlines

time (min)	d_E	d_F	d_G	d_R	d_M	d_H	d_S	d_P
k-means	2.86	24.88	5.05	3.39	1102.8	946.55	12.38	55.84
k-medoids	1.93	20.31	3.29	2.49	1036.8	884.36	12.87	43.13
AHC-single	6.51	24.91	9.46	4.21	1088.1	952.03	19.13	52.38
AHC-average	5.90	25.72	9.74	5.18	1093.2	939.87	18.31	52.53
BIRCH	7.03	28.05	-	-	1102.3	803.30	23.34	51.46
DBSCAN	6.94	26.07	6.67	4.30	1030.2	781.10	12.52	21.52
OPTICS	6.94	26.07	6.60	4.51	1029.3	780.53	13.53	43.52
SC k-means	4.84	22.77	6.34	4.77	1024.7	882.92	15.28	48.83
SC-eigen	1933.4	1327.3	1262.3	1380.5	2232.7	1953.3	1071.6	871.90
AP	95.89	116.85	94.27	111.16	1046.6	844.23	109.37	119.66
PCA	30.46	-	-	-	-	-	-	-

*Computation times for the clustering combinations include time for distance matrix due to frequent use of pair-wise similarity values in the quantitative evaluation process. The actual time for clustering algorithms themselves could be less if no distance matrix computation is required, e.g., k-means, k-medoids, BIRCH, density-based, etc..

which similarity measure ranks best for a given data set, which is similar to Xu and Chen [11] for hex-mesh quality visualization. We rank both the clustering algorithms and similarity measures w.r.t. the average value of each respective evaluation, and visualized the normalized ranking result for each data set. The clustering algorithms are sorted from top to bottom w.r.t. average evaluation index, while similarity measures are sorted from left to right w.r.t. average evaluation index as well.

The ranking visualization of streamline data sets are respectively illustrated in Fig. 3, Fig. 4, Fig. 5, Fig. 6, Fig. 7, Fig. 8, and pathline data sets are displayed in Fig. 9, Fig. 10 and Fig. 11.

6 AVERAGE EVALUATION

We simply average the evaluation results separately on streamline and pathline data sets and perform the ranking-based visualization similar to Sect. 5. The ranking visualization for streamlines and pathlines on average can be seen in Fig. 3 and Fig. 4 of the paper, while standard deviation of evaluation metrics for average streamlines is illustrated in Fig. 12.

Standard Deviation Analysis of Streamline Ranking

Since in the above matrices (see Fig. 3 in the main context), each entry is the average of six values (i.e., from six different streamline data sets), it is natural to compute the standard deviation of these six values, which describes how stable the combination

TABLE 4
Average computation time (in seconds)* for clustering techniques with various similarity measures for pathlines

time (s)	d_E	d_F	d_G	d_R	d_M	d_H	d_S	d_P	d_T
k-means	4.23	4.65	4.99	7.40	7.46	7.32	5.83	8.25	4.08
k-medoids	4.18	5.42	5.29	13.13	8.29	16.48	6.59	11.80	4.75
AHC-single	10.10	24.42	16.24	7.16	69.43	70.89	11.62	52.49	14.44
AHC-average	8.69	21.98	10.46	6.73	67.62	68.77	8.38	41.14	12.76
BIRCH	7.72	29.00	-	-	73.00	173.07	20.45	65.40	16.04
DBSCAN	2.51	16.03	1.98	2.12	61.56	62.47	2.70	49.77	6.62
OPTICS	2.50	16.01	2.53	2.31	62.09	63.79	2.71	49.75	6.62
SC k-means	5.98	19.49	5.53	5.42	64.80	65.74	6.20	35.87	10.11
SC-eigen	681.48	711.32	806.48	828.29	750.90	858.61	802.11	691.22	810.67
AP	474.72	473.39	467.57	582.92	489.51	559.09	448.79	454.94	446.10
PCA	6.48	-	-	-	-	-	-	-	-

*Computation times for the clustering combinations include time for distance matrix due to frequent use of pair-wise similarity values in the quantitative evaluation process. The actual time for clustering algorithms themselves could be less if no distance matrix computation is required, e.g., k-means, k-medoids, BIRCH, density-based, etc..

TABLE 5
Quantitative Clustering Evaluation with Different similarity Measures for Flow-Behind-Cylinder

	d_E	d_F	d_G	d_R	d_M	d_H	d_S	d_P	
k-means	0.333	0.507	0.269	0.403	0.367	0.614	0.635	0.393	0.250
	1.105	1.4e-5	2.966	1.6e-5	0.923	4.3e-3	12.95	6.6e-6	0.945
	0.335	0.359	0.300	0.270	0.361	0.541	0.582	0.166	0.355
k-medoids	0.335	0.359	0.300	0.270	0.361	0.541	0.582	0.166	0.355
	1.102	1.4e-5	2.154	1.5e-5	0.853	4.3e-3	15.851	1.2e-3	0.916
	-0.433	-0.010	-0.444	-0.009	-0.074	0.001	0.907	0.015	0.455
AHC-single	2.426	7.9e-6	2.361	7.0e-6	0.959	1.0e-3	17.82	6.3e-7	1.406
	0.316	0.512	0.250	0.418	0.382	0.628	0.784	0.543	0.325
	1.072*	1.2e-5	1.740	9.1e-6	1.041	3.6e-3	2.020*	9.8e-6	0.956
AHC-average	0.316	0.512	0.250	0.418	0.382	0.628	0.784	0.543	0.325
	1.072*	1.2e-5	1.740	9.1e-6	1.041	3.6e-3	2.020*	9.8e-6	0.956
BIRCH	0.244	0.372	0.201	0.303	-	-	-	0.233	0.291
	1.264	1.9e-5	1.598*	2.2e-5	-	-	-	1.128	1.2e-5
	-0.364	0.101	-0.261	0.037	-0.272	0.017	0.597	0.559	-0.019
DBSCAN	1.893	9.8e-6	1.608	6.1e-6	0.966	5.3e-5	315.2	1.5e-5	2.690
	-0.195	0.187	-0.248	0.090	-0.423	0.053	0.585	0.559	-0.550
OPTICS	7.048	1.2e-3	4.394	1.7e-3	1.314	7.1e-3	76.88	2.5e-3	13.97
	0.294	0.431	0.000	0.216	0.243	0.124	0.366	0.433	0.298
SC k-means	0.331	0.503	0.294	0.431	0.000	0.216	0.243	0.124	0.366
	1.095	1.4e-5	2.074	1.1e-5	1.275	1.5e-3	373.6	1.8e-3	0.922
	-0.309	0.113	-0.301	0.015	-0.432	0.021	-0.446	0.060	-0.267
SC-eigen	7.103	1.8e-3	9.946	1.6e-3	1.413	0.034	122.1	2.0e-4	8.334
	-0.713	-0.002	-0.727	0.015	-0.666	0.009	-0.333	0.031	-0.640
AP	15.17	0.038	129.8	0.025	1.199	0.076	-	1.7e-5	6.326
	0.298	0.481	-	-	-	-	-	-	4.644
PCA	1.193	2.7e-5	-	-	-	-	-	-	0.019

TABLE 6
Quantitative Clustering Evaluation with Different similarity Measures for Bernard

	d_E	d_F	d_G	d_R	d_M	d_H	d_S	d_P	
k-means	0.249	0.451	0.258	0.447	0.158	0.397	0.897	0.837	0.302
	1.334	6.8e-5	3.127*	3.3e-5	0.932	3.5e-3	1.496	3.5e-4	2.295
k-medoids	0.233	0.484	0.256	0.445	0.187	0.400	0.915	0.843	0.347
	1.503	7.4e-5	2.639	3.4e-5	0.842*	2.7e-3	1.423*	3.7e-4	2.374
	-0.427	0.005	-0.398	0.023	-0.165	0.001	0.909	0.877	-0.302
AHC-single	1.025*	3.7e-5	0.859	2.1e-5	1.008	1.1e-4	2.048	7.5e-5	0.867
	0.269	0.522	0.242	0.475	0.135	0.450	0.788	0.623	0.348
AHC-average	1.129	8.9e-5	2.257	3.2e-5	0.979	3.2e-3	2.112	2.1e-4	0.928
BIRCH	0.196	0.415	0.177	0.400	-	-	-	0.304	0.393
	1.348	3.6e-4	1.700	9.3e-5	-	-	-	1.268	1.1e-4
DBSCAN	0.261	0.434	-0.360	0.329	-0.271	0.007	0.662	0.482	-0.412
	1.422	3.8e-5	1.328	2.6e-5	1.116	3.3e-4	9.183	3.0e-9	1.422
OPTICS	-0.304	0.397	-0.326	0.162	-0.091	0.021	0.411	0.254	-0.218
	4.621	1.4e-3	4.181	2.2e-3	1.180	2.9e-3	48.99	2.1e-3	6.472
SC k-means	0.249	0.461	0.252	0.453	0.166	0.382	0.261	0.042	0.324
	1.333	7.8e-5	2.454	2.9e-5	1.050	1.4e-3	25.81	5.9e-6	2.459
SC-eigen	0.359	0.059	-0.288	0.043	-0.096	0.024	-0.705	-0.030	-0.495
	4.439	6.6e-3	8.760	6.3e-4	1.664	9.8e-3	286.0	1.9e-5	3.630
AP	-0.678	-0.024	-0.548	7.5e-3	-0.111	0.010	-0.284	0.018	-0.780
	3.141	0.012	4.511	0.044	1.452	1.8e-3	6.3e3	7.4e-6	6.453
PCA	0.243	0.365	-	-	-	-	-	-	6.223
	1.396	1.1e-4	-	-	-	-	-	-	6.707

of a clustering technique and a similarity (according to the corresponding clustering quality metric) over the six data sets. Particularly, the smaller the standard deviation, the more stable a specific combination is across the six data sets. We compute the standard deviation for all combinations, which gives rise to a number of deviation matrices w.r.t. the four quality metrics. Note that, standard deviation values are not shown for the pathline evaluation matrices since only two pathline data sets are used for our evaluation.

From the standard deviation visualization shown in Fig. 12, we see that DB index and validity measurement are quite stable across the six streamline data sets, while silhouette and Γ have quite some large variations for some combinations, which indicates that for

those combinations, the quality measured by silhouette or Γ is highly data set dependent. In particular, SC-eigen clustering seems highly dependent on the data sets when measuring its clustering quality using silhouette (Fig. 12(a)). Similarly, d_P evaluated by silhouette, d_R and d_S by Γ (Fig. 12(a)), highly depend on the data sets, despite they are ranked top among all evaluation metrics in the average quality (see Fig. 3(a)(c) in main text).

Convexity Proof of \mathbb{R}

Given a subspace $U \in \mathbb{R}$, $U = \{x \mid \|x - \bar{x}\| < \delta\}$, we need to prove that $\forall \alpha \in [0, 1], \forall x_1, x_2 \in U, \exists \hat{x} = \alpha x_1 + (1 - \alpha)x_2 \in U$. Then U is convex.

TABLE 7
Quantitative Clustering Evaluation with Different similarity Measures for **Crayfish**

	d_E	d_F	d_G	d_R	d_M	d_H	d_S	d_P
k-means	0.273 1.219	0.444 3.8e-5	0.235 1.600	0.407 5.3e-5	0.174 1.094	0.480 3.8e-3	0.452 19.40*	0.533 2.2e-6
	0.260 1.267	0.446 3.6e-5	0.239 1.435	0.418 5.6e-5	0.181 1.168	0.474 3.8e-3	0.397 70.25	0.523 2.0e-6
AHC-single	-0.239 0.900	0.078 4.3e-5	-0.428 1.003*	0.041 2.5e-5	-0.111 0.906*	0.004 1.1e-3	0.601 26.73	0.327 2.7e-6
	0.206 1.280	0.422 3.0e-5	0.232 1.642	0.433 2.8e-5	0.184 1.225*	0.556 2.5e-3	0.565 48.82	0.459 1.6e-6
AHC-average	0.229 1.147	0.354 6.8e-5	0.227 1.282	0.363 5.8e-5	- -	- -	0.269 0.997	0.313 4.8e-5
	-0.431 1.328	0.132 2.9e-5	-0.434 1.502	0.064 3.4e-5	-0.101 1.075	0.013 4.3e-4	0.362 94.04	0.484 9.4e-9
OPTICS	-0.017 4.162	0.039 0.111	-0.017 2.483	0.048 1.6e-3	-0.334 1.257	0.074 3.8e-3	0.404 21.54	0.587 1.9e-4
	0.251 1.276	0.411 3.7e-5	0.272 1.279	0.432 3.9e-5	0.131 1.173	0.354 2.0e-3	0.558 90.70	0.466 3.0e-6
SC k-means	-0.354 6.705	0.056 3.9e-3	-0.466 8.985	0.026 5.2e-3	-0.312 1.630	0.026 0.032	-0.625 49.78	0.047 2.0e-4
	0.124 1.979	0.004 1.1e-3	-0.582 2.347	0.011 5.4e-3	-0.138 1.439	0.058 7.6e-3	-0.227 152.9	0.410 4.3e-4
AP	0.264 1.236	0.442 7.6e-5	- -	- -	- -	- -	- -	- -
	- -	- -	- -	- -	- -	- -	- -	- -
PCA	0.264 1.236	- -	- -	- -	- -	- -	- -	- -

TABLE 8
Quantitative Clustering Evaluation with Different similarity Measures for **Tornado**

	d_E	d_F	d_G	d_R	d_M	d_H	d_S	d_P
k-means	0.256 1.308	0.469 1.8e-4	0.234 1.828	0.459 1.0e-4	0.285 1.015	0.518 1.8e-3	0.524 3.402	0.422 1.5e-6
	0.258 1.276	0.474 1.8e-4	0.240 1.822	0.455 1.0e-4	0.280 1.007	0.502 1.9e-3	0.572 47.32	0.531 5.4e-6
AHC-single	-0.295 1.677	-0.035 9.4e-5	-0.344 1.650	-0.028 4.0e-5	-0.043 0.000	0.000 0.855	0.471 0.423	-0.423 0.019
	0.229 1.311	0.473 1.1e-4	0.207 1.996	0.446 6.4e-5	0.218 1.133	0.523 1.8e-3	0.739 2.024	0.289 2.3e-6
AHC-average	0.229 1.311	0.473 1.1e-4	0.207 1.996	0.446 6.4e-5	0.218 1.133	0.523 1.8e-3	0.689 2.024	0.289 2.3e-6
	0.231 1.314	0.414 2.4e-4	0.212 1.621	0.431 1.6e-4	- -	- -	0.233 1.767	0.480 2.1e-5
BIRCH	-0.349 1.532	-0.107 9.1e-5	-0.341 1.414*	0.058 4.3e-5	-0.189 1.004	0.012 7.2e-5	0.491 42.17	0.670 5.6e-9
	0.193 9.650	0.049 0.084	-0.217 11.52	0.231 1.501	-0.353 0.020	0.190 492.3	-0.360 4.6e-5	0.033 2.293
OPTICS	0.244 1.322	0.524 1.7e-4	0.226 1.721	0.465 9.4e-5	0.236 1.067	0.483 4.0e-4	0.410 1.569*	0.228 8.5e-9
	0.219 1.305*	0.371 1.9e-4	0.220 1.628	0.383 1.0e-4	0.257 0.939	0.397 3.4e-4	0.483 2.473	0.188 5.6e-7
SC k-means	-0.251 1.304	0.007 0.013	-0.678 3.397	-0.021 0.025	-0.637 1.129	0.008 0.016	-0.398 3.0e+3	-0.716 9.0e-4
	0.265 1.269*	0.491 4.1e-4	- -	- -	- -	- -	- -	- -
PCA	0.265 1.269*	0.491 4.1e-4	- -	- -	- -	- -	- -	- -

TABLE 9
Quantitative Clustering Evaluation with Different similarity Measures for **Solar Plume**

	d_E	d_F	d_G	d_R	d_M	d_H	d_S	d_P
k-means	0.342 1.155	0.490 2.0e-4	0.257 1.394	0.421 2.1e-4	0.128 7.6e-3	0.397 9.068	0.476 3.4e-5	0.113 1.069
	0.342 1.134	0.490 1.9e-4	0.240 1.586	0.412 2.3e-4	0.180 1.209	0.512 6.9e-3	0.474 3.205*	0.120 1.065*
AHC-single	-0.314 1.120	0.006 1.1e-4	-0.323 0.913	0.024 8.2e-5	0.012 0.844	0.016 2.5e-3	0.937 27.75	0.972 6.6e-6
	0.306 1.064	0.640 2.1e-4	0.227 1.108	0.644 1.8e-4	0.216 1.167*	0.667 5.3e-3	0.800 81.89	0.664 7.1e-6
AHC-average	0.094 1.286	0.477 4.9e-4	0.185 1.443	0.552 8.7e-4	- -	- -	0.275 1.126	0.491 8.2e-5
	0.100 0.941*	0.439 3.9e-5	0.040 0.949	0.497 3.5e-5	-0.116 1.014	0.033 5.3e-4	0.558 27.119	0.539 4.5e-10
DBSCAN	-0.180 6.921	0.052 9.7e-3	-0.117 8.978	0.389 0.011	0.046 1.172	0.222 2.2e-3	0.359 98.95	-0.217 5.3e-5
	0.327 1.147	0.479 1.8e-4	0.237 1.572	0.401 1.6e-4	0.036 1.264	0.311 3.6e-3	0.179 38.14	0.014 1.7e-5
SC k-means	-0.553 9.145	-0.048 0.068	-0.354 8.411	0.037 0.020	-0.174 1.595	0.025 0.098	-0.786 27.67	0.058 2.0e-4
	0.010 4.248	0.068 0.060	-0.028 2.937	0.124 3.7e-3	-0.052 1.810	0.139 6.3e+3	0.327 3.7e-8	0.002 1.1e+4
AP	-0.621 4.150	-0.036 2.7e-4	-0.574 2.020	-0.021 5.3e-4	-0.077 0.898	-0.001 8.0e-3	-0.293 6.3e-3	-0.012 3.0e-5
	0.293 1.151	0.377 2.6e-4	- -	- -	- -	- -	- -	- -
PCA	0.293 1.151	0.377 2.6e-4	- -	- -	- -	- -	- -	- -

Proof

$$\begin{aligned}
 \|\hat{x} - \bar{x}\| &= \|\alpha x_1 + (1-\alpha)x_2 - \bar{x}\| \\
 &= \|x_2 - \bar{x} + \alpha(x_1 - x_2)\| \\
 &= \|\alpha(x_1 - \bar{x}) + (1-\alpha)(x_2 - \bar{x})\| \\
 &\leq \alpha\|x_1 - \bar{x}\| + (1-\alpha)\|x_2 - \bar{x}\| \\
 &< \alpha\delta + (1-\alpha)\delta \\
 &= \delta
 \end{aligned}$$

This proof can be simplified that any two points on the segment form a segment that is part of the original segment.

7 APPLICATIONS TO PARTICLE-BASED TRAJECTORY CLUSTERING

We apply the quantitative pathline evaluation results (Sect. 4.1.2 in main context) to flow trajectories from particle-based fluid simulation in Fig. 13. Since there are always more than 100,000 trajectories in fluid simulation, AHC-average/single is not applicable to trajectory clustering, and instead PCA is used. Due to memory problem for distance matrix storage, neither SC with eigen-rotation nor the hierarchical L-method can be applied to detect optimal number of clusters, hence we directly set intuitive 100 and 200 for dam-breaking and two-half-merging data sets.

TABLE 10
Quantitative Clustering Evaluation with Different similarity Measures for **Hurricane Simulation**

	d_E	d_F	d_G	d_R	d_M	d_H	d_S	d_P
k-means	0.407 1.139	0.691 2.6e-4	0.505 0.903	0.649 5.0e-5	0.014 0.015	0.258 12.130	0.650 4.7e-5	0.520 1.1e-5
	0.428 0.963	0.713 2.1e-4	0.510 0.877	0.653 5.2e-5	0.018 0.014	0.285 1.787	0.632 2.2e-4	0.591 0.736
k-medoids	0.428 0.963	0.713 2.1e-4	0.510 0.877	0.653 5.2e-5	0.018 0.014	0.285 1.787	0.632 2.2e-4	0.591 0.736
	0.169 0.743	0.132 2.3e-4	0.215 0.576*	0.090 7.0e-5	-0.015 0.950	0.005 1.6e-3	0.640 6.447	0.475 1.4e-4
AHC-single	0.169 0.743	0.132 2.3e-4	0.215 0.576*	0.090 7.0e-5	-0.015 0.950	0.005 1.6e-3	0.640 6.447	0.475 1.4e-4
	0.446 0.840	0.704 1.8e-4	0.455 0.880	0.448 1.6e-4	0.020 1.313*	0.278 7.2e-3	0.508 3.426*	0.624 7.1e-6
AHC-average	0.446 0.840	0.704 1.8e-4	0.455 0.880	0.448 1.6e-4	0.020 1.313*	0.278 7.2e-3	0.508 3.426*	0.624 7.1e-6
	0.432 0.858	0.741 4.6e-4	0.295 1.078	0.129 3.7e-4	-	-	-	-
BIRCH	0.432 0.858	0.741 4.6e-4	0.295 1.078	0.129 3.7e-4	-	-	-	-
	-0.083 0.961	0.521 3.8e-5	0.019 0.789	0.541 1.0e-5	-	-	0.264 106.7	0.626 3.6e-4
DBSCAN	0.432 0.858	0.741 4.6e-4	0.295 1.078	0.129 3.7e-4	-	-	0.264 106.7	0.626 3.6e-4
	-0.074 7.958	0.122 1.9e-3	-0.124 8.484	0.062 2.0e-3	0.010 1.889	0.066 4.5e-3	0.189 857.0	0.515 2.8e-3
OPTICS	-0.074 7.958	0.122 1.9e-3	-0.124 8.484	0.062 2.0e-3	0.010 1.889	0.066 4.5e-3	0.189 857.0	0.515 2.8e-3
	0.361 1.120	0.629 1.7e-4	0.335 1.295	0.410 4.4e-5	0.006 1.758	0.178 7.4e-3	0.207 17.18	0.238 5.8e-7
SC k-means	0.361 1.120	0.629 1.7e-4	0.335 1.295	0.410 4.4e-5	0.006 1.758	0.178 7.4e-3	0.207 17.18	0.238 5.8e-7
	0.473 0.840	0.701 1.6e-4	0.294 1.063	0.245 2.8e-5	-0.063 1.743	0.001 0.030	-0.702 27.19	0.098 2.2e-3
SC-eigen	0.473 0.840	0.701 1.6e-4	0.294 1.063	0.245 2.8e-5	-0.063 1.743	0.001 0.030	-0.702 27.19	0.098 2.2e-3
	-0.589 4.134	-0.035 6.2e-3	-0.728 4.242	-0.011 0.013	0.002 0.012	0.003 2.7e+3	-0.349 4.9e-3	0.001 4.192
AP	-0.589 4.134	-0.035 6.2e-3	-0.728 4.242	-0.011 0.013	0.002 0.012	0.003 2.7e+3	-0.349 4.9e-3	0.001 4.192
	0.558 0.682*	0.728 3.0e-4	-	-	-	-	-	-
PCA	0.558 0.682*	0.728 3.0e-4	-	-	-	-	-	-
	-	-	-	-	-	-	-	-

TABLE 11
Quantitative Clustering Evaluation with Different similarity Measures for **Cylinder Pathlines**

	d_E	d_F	d_G	d_R	d_M	d_H	d_S	d_P	d_T
k-means	0.373 1.062	0.529 1.8e-4	0.288 1.358	0.398 8.3e-5	0.048 1.913	0.350 0.014	0.740 107.5	0.447 1.9e-5	0.369 0.869
	0.368 1.053	0.511 1.8e-4	0.289 1.332	0.359 6.8e-5	0.058 1.915	0.364 0.017	0.735 3.788	0.253 2.7e-5	0.342 1.102
AHC-single	0.551 0.425	0.431 1.8e-4	0.551 0.479*	0.384 1.3e-4	0.222 1.801	0.141 0.013	0.944 0.404	0.705 4.0e-7	0.609 0.503*
	0.574 0.574	0.802 0.802	0.560 0.560	0.765 0.765	0.222 0.222	0.182 0.904	0.707 0.707	0.603 0.603	0.716 0.716
AHC-average	0.815*	2.7e-4	0.545*	8.9e-5	1.806	5.2e-3	0.975	5.4e-5	0.591
	0.521 0.796	0.800 3.3e-4	0.397 0.955	0.693 4.5e-4	-	-	-	0.354 1.061	0.481 1.388
BIRCH	0.521 0.796	0.800 3.3e-4	0.397 0.955	0.693 4.5e-4	-	-	-	0.354 0.666	0.443 0.191
	0.028 0.582	0.646 3.5e-6	-0.028 0.483	0.570 1.3e-6	-	-	0.899 8.867	0.696 8.6e-9	-0.350 1.204
OPTICS	-0.045 3.977	0.674 5.2e-3	-0.106 4.072	0.556 2.2e-3	-0.032 1.471	-0.270 6.5e-3	0.349 33.83	0.435 1.8e-4	-0.161 2.276
	0.246 1.163	0.331 7.7e-5	0.204 1.563	0.268 3.8e-5	-0.005 1.771	-0.091 0.023	0.283 36.97	0.061 1.7e-5	0.309 1.244
SC-kmeans	0.246 1.163	0.331 7.7e-5	0.204 1.563	0.268 3.8e-5	-0.005 1.771	-0.091 0.023	0.283 36.97	0.061 1.7e-5	0.309 1.244
	-0.206 6.552	0.082 3.3e-3	-0.433 7.087	0.040 4.6e-3	-0.013 1.348	-0.219 8.1e-3	-0.732 8.638	0.032 1.4e-3	-0.450 9.259
SC-eigen	0.246 6.552	0.331 3.3e-3	0.204 7.087	0.268 4.6e-3	-0.005 1.348	-0.091 8.1e-3	0.283 8.638	0.061 1.4e-3	0.309 9.259
	-0.652 4.368	0.057 2.4e-3	-0.692 11.52	-0.067 1.7e-3	-0.037 1.985	0.051 1.7e-3	-0.315 2.0e+3	0.018 1.5e-5	-0.529 6.898
AP	-0.652 4.368	0.057 2.4e-3	-0.692 11.52	-0.067 1.7e-3	-0.037 1.985	0.051 1.7e-3	-0.315 2.0e+3	0.018 1.5e-5	-0.529 6.898
	0.304 1.101	0.430 2.8e-4	-	-	-	-	-	-	-

TABLE 12
Quantitative Clustering Evaluation with Different similarity Measures for **Tube Pathlines**

	d_E	d_F	d_G	d_R	d_M	d_H	d_S	d_P	d_T
k-means	0.357 0.986	0.517 5.6e-5	0.342 1.427	0.471 1.9e-5	0.269 0.442	0.496 2.7e-4	0.370 0.927	0.501 9.8e-5	-
	0.331 0.992	0.497 5.5e-5	0.334 1.379	0.483 2.8e-5	0.262 0.459	0.472 2.4e-4	0.343 1.020	0.502 1.8e-4	0.370 0.945
AHC-single	-0.010 1.660	0.193 2.3e-5	0.055 3.135	0.442 9.2e-6	-0.021 0.404	0.497 1.3e-4	0.544 10.49	0.358 2.3e-6	-0.156 1.789
	0.305 0.962*	0.523 5.6e-5	0.317 1.380	0.481 1.3e-5	0.228 0.451	0.574 2.5e-4	0.552 27.66	0.553 2.3e-6	-0.038 1.347
AHC-average	0.313 0.991	0.529 6.7e-5	0.265 1.469	0.460 4.2e-5	-	-	0.350 -	0.442 -	0.493 1.347
	0.009 1.761	0.215 5.7e-6	0.172 1.345	0.304 1.6e-6	0.086 0.404	0.501 4.0e-5	0.208 238.2	0.564 4.4e-8	-0.223 1.332
BIRCH	0.313 0.991	0.529 6.7e-5	0.265 1.469	0.460 4.2e-5	-	-	0.350 -	0.442 -	0.493 1.347
	0.009 1.761	0.215 5.7e-6	0.172 1.345	0.304 1.6e-6	0.086 0.404	0.501 4.0e-5	0.208 238.2	0.564 4.4e-8	-0.223 1.332
DBSCAN	0.300 -0.140	0.474 0.101	0.323 -0.158	0.468 0.149	0.235 0.068	0.460 0.169	0.501 0.131	0.438 0.374	-0.284 -0.284
	1.099 -0.462	0.474 0.024	1.303* -0.276	0.323 0.063	0.225 -0.337	0.460 0.028	0.501 -0.597	0.438 -0.057	-0.284 -0.284
OPTICS	0.300 1.099	0.474 3.6e-5	0.323 1.303*	0.468 1.2e-5	0.235 0.466	0.460 2.7e-4	0.501 272.0	0.438 6.8e-7	-0.284 -0.284
	0.445 -0.511	0.445 0.034	5.822 -0.664	1.4e-3 -0.001	0.235 0.212	0.460 0.202	0.501 -0.585	0.438 0.065	-0.284 -0.284
SC-kmeans	0.348 4.776	0.494 1.1e-4	-	-	-	-	-	-	-
	0.976	0.494	-	-	-	-	-	-	-
SC-eigen	0.348 4.776	0.494 1.1e-4	-	-	-	-	-	-	-
	0.976	0.494	-	-	-	-	-	-	-
AP	0.348 4.776	0.494 1.1e-4	-	-	-	-	-	-	-
	0.976	0.494	-	-	-	-	-	-	-
PCA	0.348 0.976	0.494 1.1e-4	-	-	-	-	-	-	-

The detailed discussion of PCA and k-means with d_G for these two particle-based flow trajectory clustering results can be also referenced in Shi and Chen [2].

8 VISUAL INSPECTION

We provide the segmentation results for blood flow in Fig. 14 and additional pathline abstraction results in Fig. 15. For blood flow segmentation, We notice that AHC-average with spatial similarity measures (d_E , d_M , d_H and d_T) can generate better pathline bundling than PCA (not coherent clusters generated). For pathline abstraction, we note that due to its simplicity and clear features, almost every abstraction preserves good features for blood flow, while only

AHC-average with d_S (see Fig. 15(d)) shows better abstraction for cylinder pathlines.

9 COMMENT ON SC IN FLOW VISUALIZATION

To our best knowledge, the only application of SC in simulation flow data sets is in streamline embedding [3] (TVCG 2012) for better illustration of streamline clustering results in representation of 3D spectral embedding space. Afterwards, we have not found further applications of SC in other flow data sets except blood flow. From our comparative evaluation, we can find some reasons (detailed below) that restrict the applications of SC in flow visualization:

TABLE 13
Quantitative Clustering Evaluation with Different similarity Measures for **Blood Flow**

	d_E	d_F	d_G	d_R	d_M	d_H	d_S	d_P	d_T									
k-means	0.388 1.103	0.773 1.4e-3	0.393 1.320	0.601 5.2e-4	-0.001 2.448	0.156 0.033	0.664 1.012*	0.848 0.010	- -	0.496 1.686	0.652 8.5e-4	-0.508 26.27	-0.175 7.6e-7	- -	-	0.514 0.969	0.787 5.4e-4	
	0.388 1.102	0.772 1.4e-3	0.423 1.228	0.615 3.1e-4	-0.000 0.236	0.191 0.029	0.673 1.560	0.840 0.013	- -	0.493 1.682*	0.632 7.8e-4	-0.389 39.11	-0.094 8.8e-8	- -	-	0.474 1.071	0.747 7.7e-4	
AHC-single	0.393 0.976	0.790 9.8e-4	0.103 1.140	0.156 1.4e-4	-0.001 1.919*	0.088 9.1e-4	0.609 345.4	0.755 2.6e-5	0.382 0.431	0.464 4.663	0.535 3.9e-4	0.811 8.293	0.379 2.0e-3	0.306 1.191*	-0.685 4.6e-13	0.147 0.984	0.047 5.8e-4	
	0.386 1.037	0.794 9.5e-4	0.475 1.248	0.711 3.1e-4	0.021 2.100*	0.552 0.012	0.710 256.0	0.703 2.8e-5	0.739 0.469	0.902 1.0e-4	0.610 6.287	0.859 7.819	0.519 2.6e-3	0.715 24.91	0.355 3.1e-9	0.508 0.020	0.833 5.2e-4	
BIRCH	0.280 1.288	0.773 1.6e-3	0.326 1.631	0.615 8.0e-4	- -	- -	0.640 0.573	0.278 3.3e-4	0.039 2.864	0.548 0.015	0.278 0.015	0.267 0.015	- -	-	0.421 1.017	0.796 8.7e-4		
	0.050 1.059	0.658 3.3e-4	0.558 0.755*	0.696 3.8e-5	-0.473 -	0.432 -	0.709 173.2	0.431 5.3e-8	0.309 4.402	0.329 16.99	0.371 2.6e-5	0.495 22.27	0.381 1.7e-4	0.550 -	- -	0.330 1.071	0.721 2.3e-4	
OPTICS	-0.003 1.635	0.032 0.016	0.014 2.232	0.105 5.7e-3	-0.002 2.333	-0.174 6.1e-3	0.086 18.82	0.276 1.8e-4	-0.204 4.851	0.431 0.027	-0.014 9.349	0.276 0.019	0.259 4.150*	0.213 2.3e-3	- -	-0.017 1.654	0.019 4.8e-3	
	0.373 1.185	0.761 1.7e-3	0.371 1.302	0.564 2.7e-4	0.012 0.237	0.395 0.021	0.640 4.412	0.579 2.2e-5	0.648 0.931	0.341 5.0e-5	0.389 10.26	0.589 1.5e-3	0.196 7.133	0.202 1.2e-3	-0.022 32.42	0.105 7.4e-10	0.470 1.066	0.745 5.7e-4
SC-kmeans	0.417 1.031	0.794 1.2e-3	-0.344 3.588	0.088 8.7e-3	-0.026 2.693	0.035 0.066	0.117 8.357	0.247 6.1e-4	0.789 0.442*	0.908 3.9e-5	0.481 2.828	0.660 7.5e-4	0.225 4.706	0.085 6.1e-4	0.125 19.96	0.222 8.4e-11	0.560 0.892*	0.817 4.0e-4
	-0.070 2.885	0.108 4.2e-3	0.284 1.916	0.355 9.4e-4	- -	- -	-0.183 173.5	0.050 3.6e-3	-0.554 3.222	0.051 3.8e-3	-0.378 0.253	0.002 -	- -	- -	-	0.073 5.392	0.094 1.9e-3	
PCA	0.337 1.246	0.731 3.7e-3	- -	- -	- -	- -	- -	- -	- -	- -	- -	- -	- -	- -	- -	- -	- -	

TABLE 14
Quantitative Clustering Evaluation of Single-Level Affinity Propagation on Different Data Sets with Different Similarity Measures

	d_E	d_F	d_G	d_R	d_M	d_H	d_S	d_P	d_T									
Cylinder	0.074 5.3e3	0.057 3.0e-5	-0.023 1.0e4	0.041 6.2e-5	0.060 0.665	0.082 9.6e-4	0.021 -	0.00083 -	0.131 24.20	0.062 5.6e-6	-0.029 3.6e3	0.059 1.3e-4	0.139 9.025	0.0075 4.7e-6	-0.496 50.50	-0.012 4.3e-7	- -	- -
	0.058 1.505	0.050 1.0e-4	-0.066 1.986	0.080 3.1e-8	0.103 0.869	0.184 3.2e-3	0.332 8.9e3	-0.00022 1.7e-7	0.059 2.278	0.113 1.5e-5	0.077 2.703	0.161 4.9e-4	0.015 6.467	- -	- -	- -	- -	
Crayfish	0.034 1.586	0.128 1.5e-4	-0.010 1.709	0.105 1.4e-4	0.042 0.943	0.187 5.2e-3	0.224 7.122	0.435 7.7e-7	0.029 1.611	0.131 5.1e-5	0.051 1.828	0.144 2.6e-4	0.033 2.988	0.157 1.9e-4	- -	- -	- -	- -
	0.028 1.564	0.076 1.4e-4	-0.0057 1.639	0.055 1.2e-4	0.057 0.621	0.095 1.1e-4	0.330 -	0.0055 4.2e-9	0.096 1.438	0.056 1.2e-4	0.035 1.950	0.092 4.1e-4	0.092 66.24	0.0074 8.1e-7	-0.332 302.2	0.023 3.2e-5	- -	- -
Solar Plume	0.010 1.550	0.068 2.7e-4	-0.028 2.020	0.124 5.3e-4	-0.052 0.898	0.139 8.0e-3	0.327 6.3e3	-0.00028 3.7e-8	0.027 1.902	0.113 1.2e-4	0.077 1.938	0.142 7.5e-4	0.015 115.2	0.027 1.0e-7	-0.046 322.6	0.028 1.3e-6	- -	- -
	0.0028 1.852	0.104 3.5e-4	-2.7e-3 1.546	0.109 9.1e-5	-0.096 1.559	0.078 0.123	0.021 1.8e3	0.078 2.8e-10	-0.043 2.733	0.099 1.4e-5	0.027 3.146	0.113 4.5e-4	-0.049 12.93	-0.019 1.7e-4	-0.687 36.05	-0.019 3.2e-5	- -	- -
Tube Pathlines	0.119 1.838	0.174 7.4e-5	0.011 3.7/4	0.115 1.3e-4	0.113 0.220	0.184 8.0e-4	0.345 1.1e3	0.065 6.2e-8	0.178 2.098	0.115 6.1e-6	0.033 3.076	0.186 6.4e-4	0.090 17.51	0.187 3.0e-3	-0.192 7.761	0.153 0.039	0.054 2.832	0.171 8.2e-5
	0.212 9.428	0.043 1.5e-5	0.024 16.40	0.042 6.2e-5	0.271 1.926	0.057 2.6e-4	0.335 1.1e3	0.023 5.6e-7	0.022 1.806	0.176 5.2e-5	0.194 10.63	0.027 1.0e-5	0.027 616.4	0.044 1.2e-5	- -	-	0.101 12.90	0.069 1.2e-5
Cylinder Pathlines	0.172 1.368	0.360 179	0.155 1203	0.392 100	-0.0011 1304	0.247 374	0.377 1949	0.115 1101	0.0025 445	0.224 39	0.206 1518	0.315 343	0.061 1144	0.355 96	-0.986 1	0.218 2	0.106 214	0.307 627
	0.32 1.507	32 3	14 2	29 1	343 2.121	197 0.017	310.2 4.656	1.5e-7 4.4e-4	73 11.25	3 7.3e-4	171 24.26	5 6.9e-3	19 1.9e10	1 1.5e-4	24 1	32 2	-	-

The affinity propagation (AP) in this table is single-level different from the hierarchical (two-level) AP used by Tao et al. [5], [6].

TABLE 15
Number of clusters with single-level (left) and two-level (right) affinity propagation (AP) for the 9 experimental data sets

	d_E	d_F	d_G	d_R	d_M	d_H	d_S	d_P	d_T									
Flow behind cylinder	3544 2614	442 42	4107 1616	696 34	2369 281	238 4	6721 5314	3688 3216	3603 2303	742 127	2349 1588	138 34	6087 4156	2722 1913	2286 1	49 1	- -	- -
	605 3115	3 6	969 4020	20 147	127 2781	6 187	917 5148	198 2030	841 4599	4 18	503 1570	8 2	4156 3020	1913 1125	1024 772	255 1	- -	- -
Hurricane	880 1111	37 32	1851 656	193 26	576 379	2 4	5341 3573	2902 2131	1243 741	50 11	926 184	8 4	4156 2869	1913 1110	1024 2	255 1	- -	- -
	1368 567	179 47	1203 827	100 142	1304 212	374 2	1949 1366	1101 373	445 984	39 266	1518 423	343 1	1144 63	96 2	1024 214	255 2	627 627	48 48
Blood Flow	32 1.507	3 3.3e-3	14 2.160	2 8.5e-4	29 2.121	1 0.017	343 4.656	197 4.4e-4	73 11.25	3 7.3e-4	171 24.26	5 6.9e-3	19 1.9e10	1 1.5e-4	24 1	32 2	-	-

- SC for spatial clustering of streamlines in flow data sets **does not show better visualization** than, especially, the hierarchical clustering methods, either quantitatively (see the evaluation metric tables for different flow data sets in the paper) or qualitatively (see spatial clustering examples for Bernard simulation flows in Fig. 2).
- Compared to hierarchical clustering, SC requires **more computational resources** especially for matrix eigen-decomposition, and for the SC-eigen it always takes much longer time for the optimal search of the minimal eigen-rotation (see Tables 3 and 4).
- SC requires to set more parameters (i.e. number of clusters, Gaussian kernel radius, number of smallest eigenvalues, and post-processing after eigen-decomposition), and it is often **impractical for interactive exploration** with different parameters. For example, in k-way normalized or SC eigen-minimization, if k (i.e. the number of preset clusters) is changed, the final optimal clusters have to be re-computed with specific minimization. This is not convenient for interaction when compared to AHC in which once bottom-up hierarchical tree is built different number of clusters can be traversed along different level of the tree without extra calculation.
- SC-eigen is used to find the optimal number of clusters given a specific bound k so that the optimal number of clusters is searched in the range $[2,k]$. This is practical only when the k is not too big or is known, e.g., in the blood flow application [15], [16] k is not larger than 20 with a-priori knowledge. However, for complicated CFD simulation data sets, the optimal value of k is often unknown, thus k is often set to some big values (e.g., more than 100). We already see the huge computational time required for SC-eigen with $k=100$ for simulated flows (see Table. 3). Hence, **SC-eigen is not well applicable and practical for scientific simulation data sets**.
- We searched all the papers related to SC in flow visualization, and found **SC can only be compatible with spatial similarity distances**, e.g., MCP, Hausdorff distance, min-

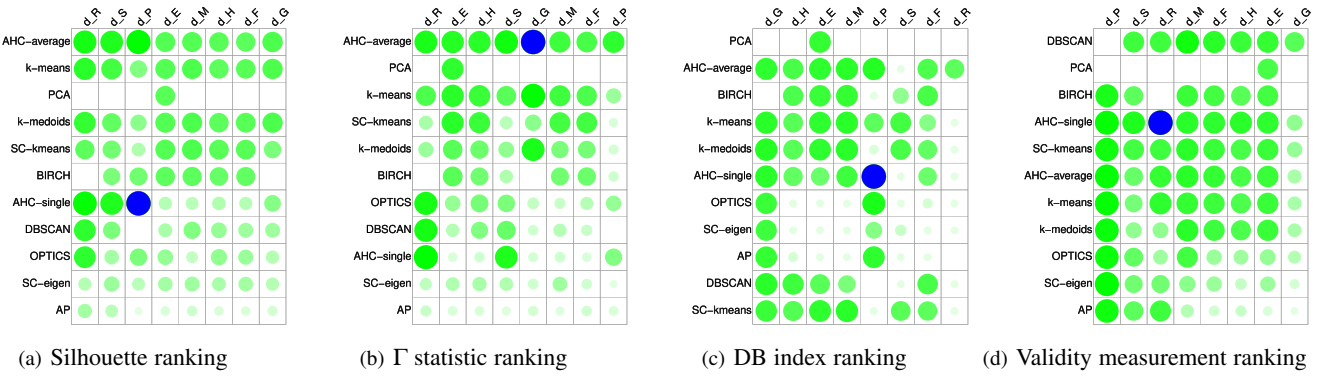


Fig. 3. Evaluation ranking visualization for streamline **cylinder** data set with blue highlighting best evaluation combination with respect to the four clustering quality metrics. Fig. 3(a) indicates that single-linkage AHC combined with $d_P(\cdot, \cdot)$ has the highest silhouette value for the cylinder data, Fig. 3(b) indicates average-linkage AHC and $d_G(\cdot, \cdot)$ has the highest Γ statistics, Fig. 3(c) shows single-linkage AHC and $d_P(\cdot, \cdot)$ exhibits the lowest DB index, and Fig. 3(d) demonstrates single-linkage AHC and $d_R(\cdot, \cdot)$ exhibits the lowest validity measurement.

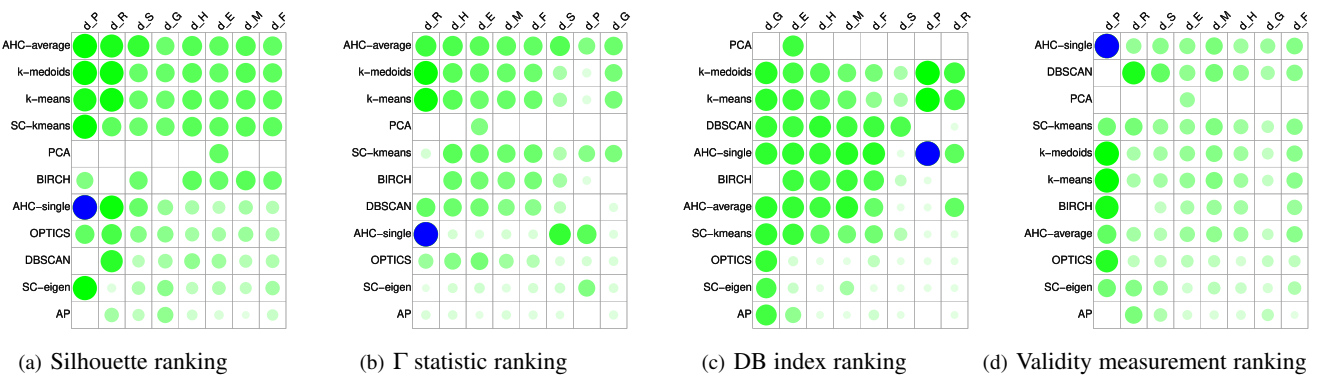


Fig. 4. Evaluation ranking visualization for streamline **bernard** data set with blue circle highlighting best evaluation combination. Fig. 4(a) indicates that single-linkage AHC combined with $d_P(\cdot, \cdot)$ has the highest silhouette value, Fig. 4(b) indicates single-linkage AHC and $d_R(\cdot, \cdot)$ has the highest Γ statistics, Fig. 4(c) shows single-linkage AHC coupled with $d_P(\cdot, \cdot)$ has the lowest DB index, and Fig. 4(d) demonstrates single-linkage AHC combined with $d_P(\cdot, \cdot)$ has the lowest validity measurement.

imal closest point distance, etc.. On the other hand, more attention is now paid to the shape-based similarity measures since flow features are often highlighted or bounded by specific shapes of streamlines/pathlines, and customized similarity measures are easier to be coupled with AHC and users can even edit the linkage types (see Sect. 2.2 in the paper).

ACKNOWLEDGMENTS

This work is supported by National Science Foundation (IIS 1553329). We would like to thank the anonymous reviewers of IEEE VIS 2018 and TVCG for providing instructive comments to our work. We also wish to thank Duong Binh Nguyen for providing the streamline and pathline data sets.

REFERENCES

- [1] C. C. Aggarwal, A. Hinneburg, and D. A. Keim, “On the surprising behavior of distance metrics in high dimensional spaces,” in *Proceedings of the 8th International Conference on Database Theory*, ser. ICDT ’01. London, UK, UK: Springer-Verlag, 2001, pp. 420–434. [Online]. Available: <http://dl.acm.org/citation.cfm?id=645504.656414>
- [2] L. Shi and G. Chen, “Metric-based curve clustering and feature extraction in flow visualization,” in *2017 IEEE Conference on Computer-Aided Design and Computer Graphics short paper*, 2017.
- [3] C. Rossel and H. Theisel, “Streamline embedding for 3d vector field exploration,” *IEEE Transactions on Visualization and Computer Graphics*, vol. 18, no. 3, pp. 407–420, March 2012.
- [4] T. McLoughlin, M. W. Jones, R. S. Laramee, R. Malki, I. Masters, and C. D. Hansen, “Similarity measures for enhancing interactive streamline seeding,” *IEEE Transactions on Visualization and Computer Graphics*, vol. 19, no. 8, pp. 1342–1353, Aug 2013.
- [5] J. Tao, C. Wang, and C. K. Shene, “Flowstring: Partial streamline matching using shape invariant similarity measure for exploratory flow visualization,” in *2014 IEEE Pacific Visualization Symposium*, March 2014, pp. 9–16.
- [6] J. Tao, C. Wang, C. K. Shene, and R. A. Shaw, “A vocabulary approach to partial streamline matching and exploratory flow visualization,” *IEEE Transactions on Visualization and Computer Graphics*, vol. 22, no. 5, pp. 1503–1516, May 2016.
- [7] D. G. Kendall, “A survey of the statistical theory of shape,” *Statistical Science*, vol. 4, no. 2, pp. 87–99, 1989. [Online]. Available: <http://www.jstor.org/stable/2245331>
- [8] M. Meuschke, S. Voß, B. Preim, and K. Lawonn, “Exploration of blood flow patterns in cerebral aneurysms during the cardiac cycle,” *Computers & Graphics*, vol. 72, pp. 12 – 25, 2018. [Online]. Available: <http://www.sciencedirect.com/science/article/pii/S0097849318300128>
- [9] M. Meuschke, S. Oeltze-Jafra, O. Beuing, B. Preim, and K. Lawonn, “Classification of blood flow patterns in cerebral aneurysms,” *IEEE Transactions on Visualization and Computer Graphics*, pp. 1–1, 2018.
- [10] B. J. Frey and D. Dueck, “Clustering by passing messages between data points,” *Science*, vol. 315, no. 5814, pp. 972–976, 2007. [Online]. Available: <http://science.sciencemag.org/content/315/5814/972>
- [11] K. Xu and G. Chen, “Hexahedral mesh structure visualization and evaluation,” *IEEE Transactions on Visualization and Computer Graphics*, vol. 25, no. 1, pp. 1173–1182, Jan 2019.

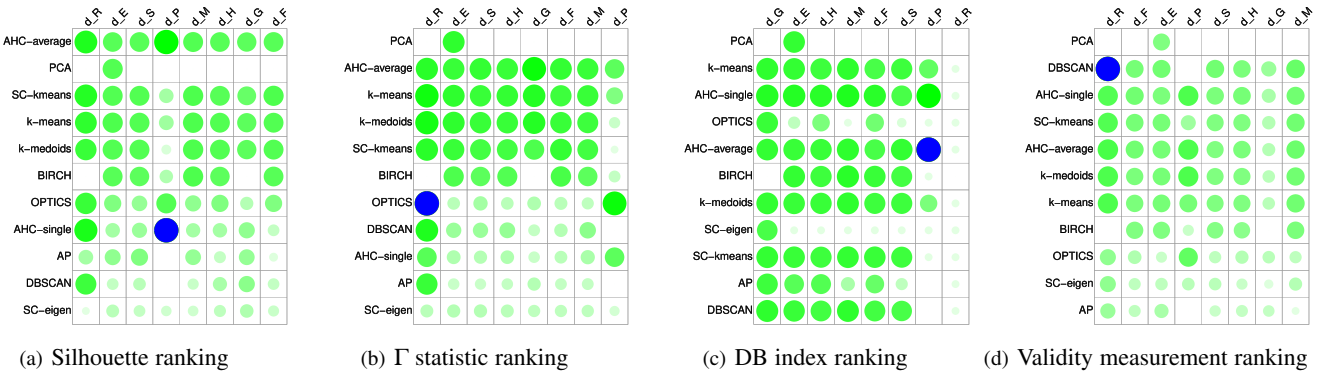


Fig. 5. Evaluation ranking visualization for streamline **crayfish** data set with blue highlighting best evaluation combination. Fig. 5(a) indicates that single-linkage AHC combined with $d_P(\cdot, \cdot)$ has the highest silhouette value, Fig. 5(b) indicates OPTICS and $d_R(\cdot, \cdot)$ has the highest Γ statistics, Fig. 5(c) shows average-linkage AHC and $d_P(\cdot, \cdot)$ has the lowest DB index, and Fig. 5(d) demonstrates DBSCAN and $d_R(\cdot, \cdot)$ has the lowest validity measurement.

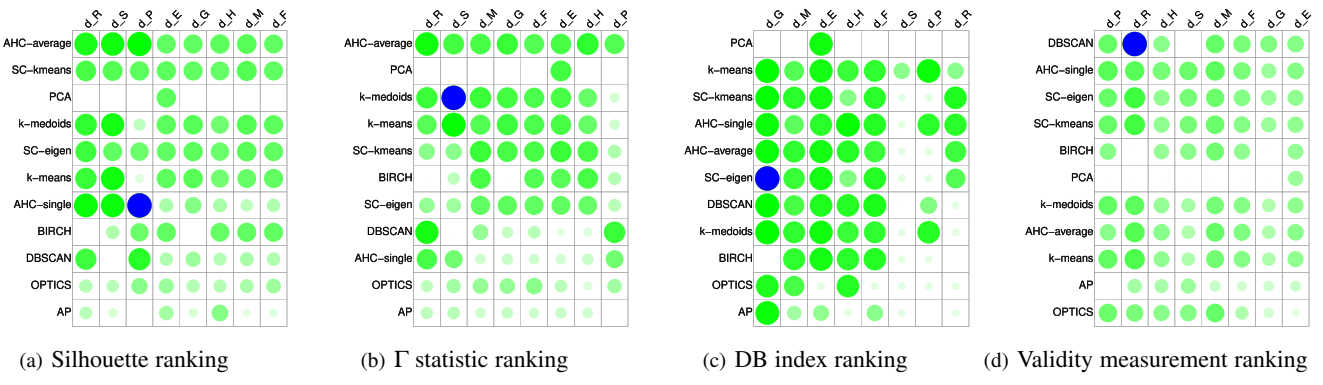


Fig. 6. Evaluation ranking visualization for streamline **tornado** data set with blue highlighting best evaluation combination. Fig. 6(a) indicates that single-linkage AHC coupled with $d_P(\cdot, \cdot)$ has the highest silhouette values, Fig. 6(b) indicates k-medoids combined with $d_S(\cdot, \cdot)$ has the highest Γ statistics, Fig. 6(c) shows SC-eigen combined with $d_G(\cdot, \cdot)$ exhibits the lowest DB index, and Fig. 6(d) demonstrates DBSCAN + $d_R(\cdot, \cdot)$ exhibits the lowest validity measurement.

- [12] M. Macklin and M. Müller, “Position based fluids,” *ACM Trans. Graph.*, vol. 32, no. 4, pp. 104:1–104:12, Jul. 2013. [Online]. Available: <http://doi.acm.org/10.1145/2461912.2461984>
- [13] N. Akinci, M. Ihmsen, G. Akinci, B. Solenthaler, and M. Teschner, “Versatile rigid-fluid coupling for incompressible sph,” *ACM Trans. Graph.*, vol. 31, no. 4, pp. 62:1–62:8, Jul. 2012. [Online]. Available: <http://doi.acm.org/10.1145/2185520.2185558>
- [14] N. Kang and D. Sagong, “Incompressible sph using the divergence-free condition,” *Computer Graphics Forum*, vol. 33, no. 7, pp. 219–228, 2014. [Online]. Available: <http://dx.doi.org/10.1111/cgf.12490>
- [15] S. Oeltze, D. J. Lehmann, H. Theisel, and B. Preim, “Evaluation of streamline clustering techniques for blood flow data,” 2012.
- [16] S. Oeltze, D. J. Lehmann, A. Kuhn, G. Janiga, H. Theisel, and B. Preim, “Blood flow clustering and applications in virtual stenting of intracranial aneurysms,” *IEEE Transactions on Visualization and Computer Graphics*, vol. 20, no. 5, pp. 686–701, May 2014.

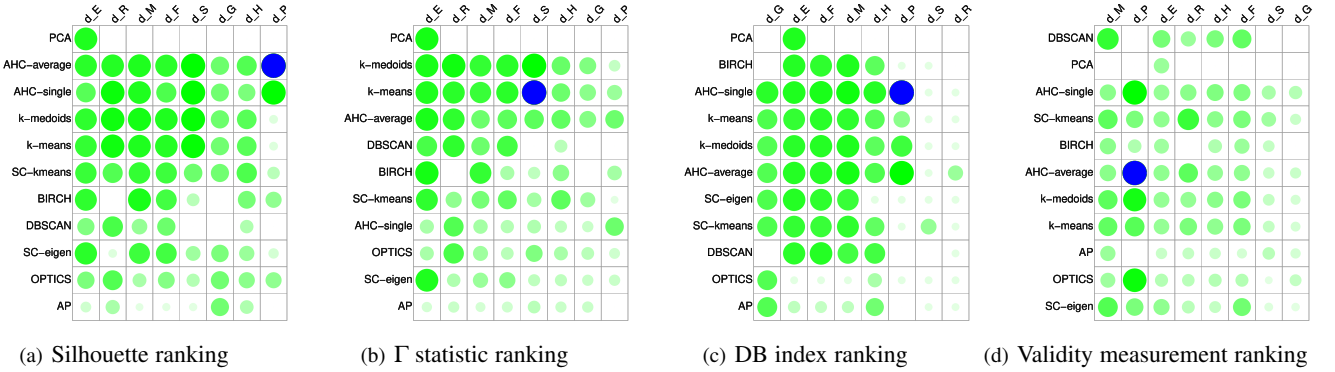


Fig. 7. Evaluation ranking visualization for streamline **hurricane** data set with blue highlighting best evaluation combination. Fig. 7(a) indicates that average-linkage combined with $d_P(\cdot, \cdot)$ has the highest silhouette values, Fig. 7(b) indicates k-means and $d_S(\cdot, \cdot)$ has the highest Γ statistics, Fig. 7(c) shows single-linkage AHC + $d_P(\cdot, \cdot)$ has the lowest DB index, and Fig. 7(d) demonstrates average-linkage AHC + $d_P(\cdot, \cdot)$ has the lowest validity measurement.

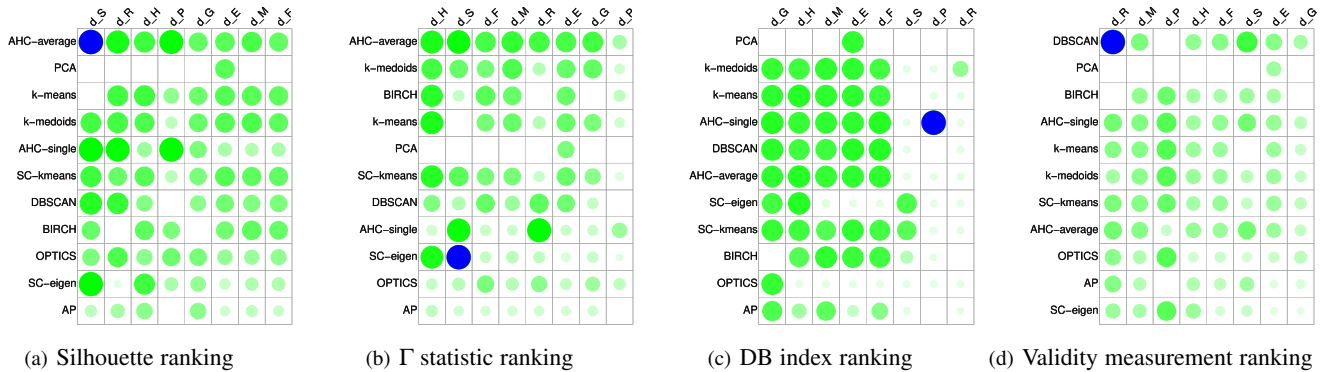


Fig. 8. Evaluation ranking visualization for streamline **solar plume** data set with blue highlighting best evaluation combination. Fig. 8(a) indicates that average-linkage AHC combined with $d_S(\cdot, \cdot)$ has the highest silhouette values, Fig. 8(b) indicates SC-eigen coupled with $d_S(\cdot, \cdot)$ has the highest Γ statistics, Fig. 8(c) shows single-linkage AHC + $d_P(\cdot, \cdot)$ exhibits the lowest DB index, and Fig. 8(d) demonstrates the combination of DBSCAN and $d_R(\cdot, \cdot)$ exhibits the lowest validity measurement.

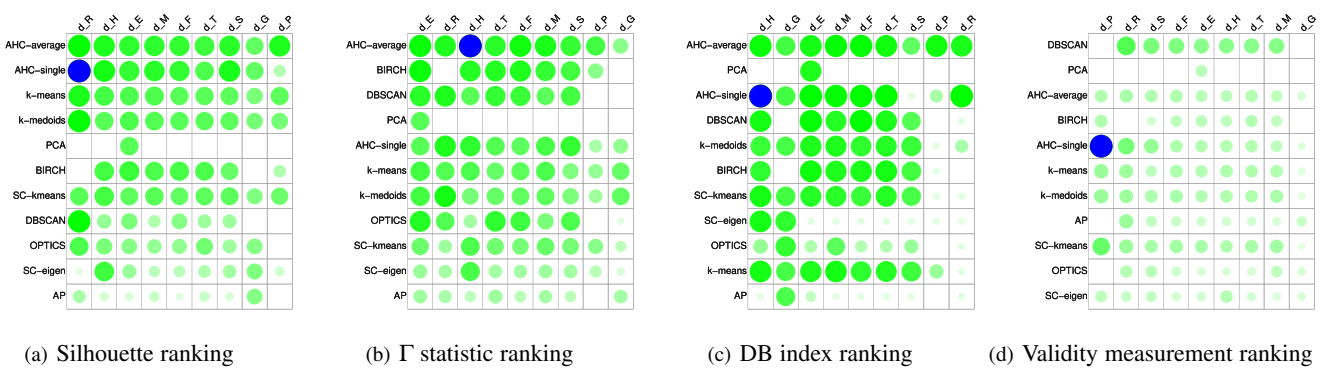


Fig. 9. Evaluation ranking visualization for **cylinder pathline** data set with blue highlighting best evaluation combination. Fig. 9(a) indicates that the combination of single-linkage AHC and $d_R(\cdot, \cdot)$ has the highest silhouette values, Fig. 9(b) indicates average-linkage AHC combined with $d_H(\cdot, \cdot)$ has the highest Γ statistics, Fig. 9(c) shows single-linkage AHC coupled with $d_H(\cdot, \cdot)$ exhibits the lowest DB index, and Fig. 9(d) demonstrates single-linkage AHC + $d_P(\cdot, \cdot)$ exhibits the lowest validity measurement.

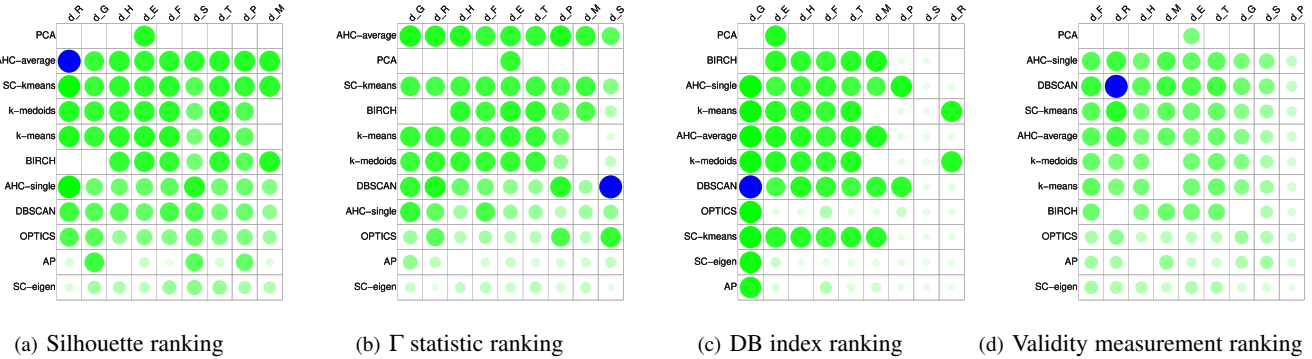


Fig. 10. Evaluation ranking visualization for **tube pathline** data set with blue highlighting best evaluation combination. Fig. 10(a) indicates that average-linkage AHC combined with $d_R(\cdot, \cdot)$ has the highest silhouette values, Fig. 10(b) indicates the combination of DBSCAN and $d_S(\cdot, \cdot)$ has the highest Γ statistics, Fig. 10(c) shows DBSCAN coupled with $d_G(\cdot, \cdot)$ exhibits the lowest DB index, and Fig. 10(d) demonstrates that DBSCAN + $d_R(\cdot, \cdot)$ exhibits the lowest validity measurement.

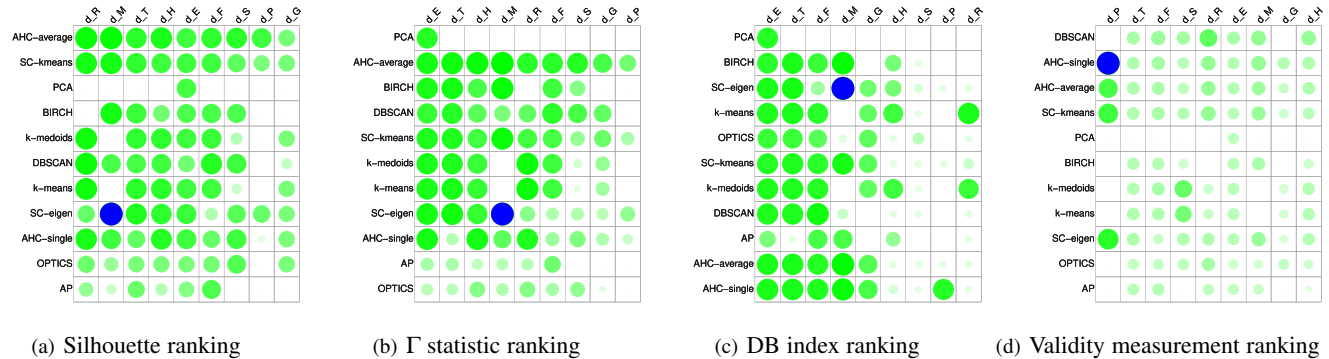


Fig. 11. Evaluation ranking visualization for **blood flow** data set with blue highlighting best evaluation combination. Fig. 11(a) indicates that the combination of SC-eigen and $d_M(\cdot, \cdot)$ has the highest silhouette value, Fig. 11(b) indicates SC-eigen coupled with $d_M(\cdot, \cdot)$ has the highest Γ statistics, Fig. 11(c) shows SC-eigen combined with $d_M(\cdot, \cdot)$ exhibits the lowest DB index on average, and Fig. 11(d) demonstrates single-linkage AHC + $d_P(\cdot, \cdot)$ exhibits the lowest validity measurement.

TABLE 16

Quantitative Clustering Evaluation with Different similarity Measures for Streamline Data Sets on Average

TABLE 17
Quantitative Clustering Evaluation with Different similarity Measures for Pathline Data Sets on Average

	d_E	d_F	d_G	d_R	d_M	d_H	d_S	d_P	d_T
k-means	0.373	0.606	0.341	0.490	0.105	0.334	0.591	0.599	0.369
	1.050	5.5e-4	1.368	2.1e-4	1.601	0.016	36.48	3.5e-3	0.869
k-medoids	0.362	0.594	0.348	0.486	0.107	0.343	0.641	0.692	0.356
	1.049	5.5e-4	1.313	1.3e-4	1.580	0.015	2.122*	4.3e-3	1.201*
AHC-single	0.311	0.471	0.236	0.328	0.067	0.242	0.699	0.606	0.278
	1.020	3.9e-4	0.978	9.3e-5	1.374	4.6e-3	118.8	9.7e-6	0.996
AHC-average	0.421	0.707	0.451	0.652	0.157	0.436	0.722	0.654	0.561
	0.938	4.3e-4	1.058	1.4e-4	1.452 *	5.7e-3	94.87	2.8e-5	0.655
BIRCH	0.371	0.700	0.330	0.589	-	-	0.448	0.630	0.252
	1.025	6.5e-4	1.351	4.3e-4	-	-	0.847	3.4e-4	1.841
DBSCAN	0.029	0.500	0.234	0.523	-0.194	0.466	0.605	0.564	-0.088
	1.134	1.1e-4	0.860	1.4e-5	0.244*	4.0e-5	140.1	3.5e-8	2.313
OPTICS	-0.063	0.269	-0.083	0.270	0.012	-0.092	0.189	0.361	-0.216
	3.637	9.5e-3	3.402	3.4e-3	1.400	4.5e-3	106.0	2.4e-4	4.245
SC-kmeans	0.306	0.522	0.299	0.433	0.081	0.255	0.475	0.359	0.431
	1.149	6.0e-4	1.389	1.1e-4	1.491	0.015	104.5	1.3e-5	1.117
SC-eigen	-0.084	0.300	-0.351	0.064	-0.125	-0.052	-0.404	0.074	0.195
	4.010	2.3e-3	5.499	4.9e-3	1.557	0.033	90.96	1.5e-3	5.276
AP	-0.411	0.067	-0.358	0.096	0.087	0.126	-0.361	0.044	-0.571
	4.010	7.6e-3	5.799	1.4e-3	1.392	2.2e-3	1.1e+3	2.0e-3	4.867
PCA	0.330	0.551	-	-	-	-	-	-	-
	1.108	1.4e-3	-	-	-	-	-	-	-

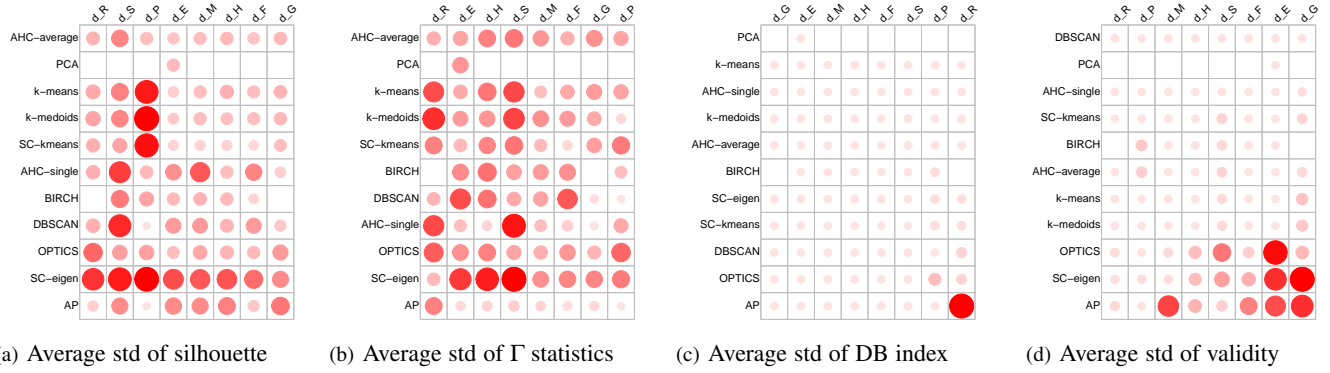


Fig. 12. Visualization of the standard deviation of the average of the quality matrices for the 6 streamline data sets. The more saturated and larger the red dot, the larger the deviation. As we see, most entries have very small standard deviation values for the DB index and validity metrics, indicating that they are quite stable across the 6 streamline data sets. For the silhouette metric, it shows that SC-eigen clustering and the d_P and d_S are the most unstable for the 6 data sets. For the Γ statistics metric, the standard deviation values are relatively large in many cases, indicating that this metric can be highly data set dependent, thus not a very reliable one.

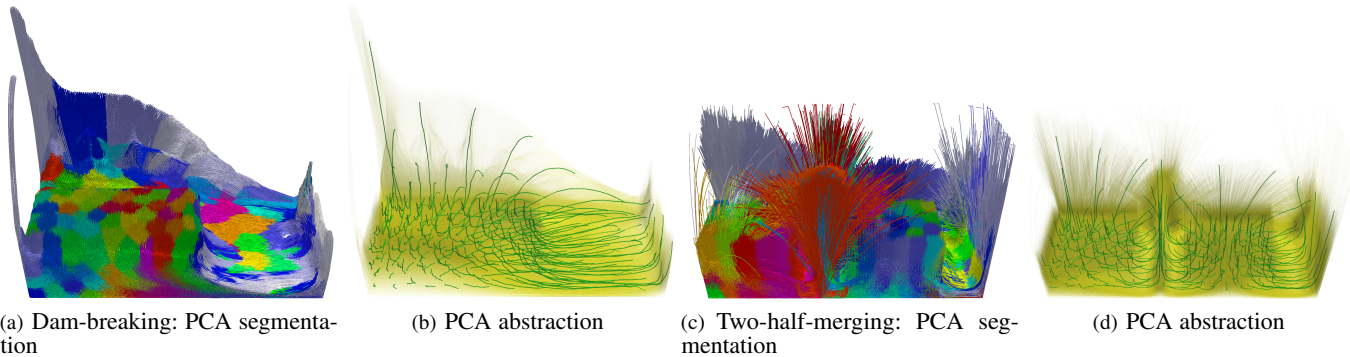


Fig. 13. PCA-based segmentation and abstraction for particle-based trajectories from the position-based fluid simulations [12]. (a-b): dam-breaking (128K trajectories within frame 50 and 300) with signed-distance boundary handling. (c-d): two-half-merging (300K trajectories within frame 100 and 350) with boundary-particle handling [13] and free-slip condition [14]. Time step of 0.016s is set for both simulations as required in [12]. 100 and 200 clusters are set for the dam-breaking and two-half-merging data sets, respectively.

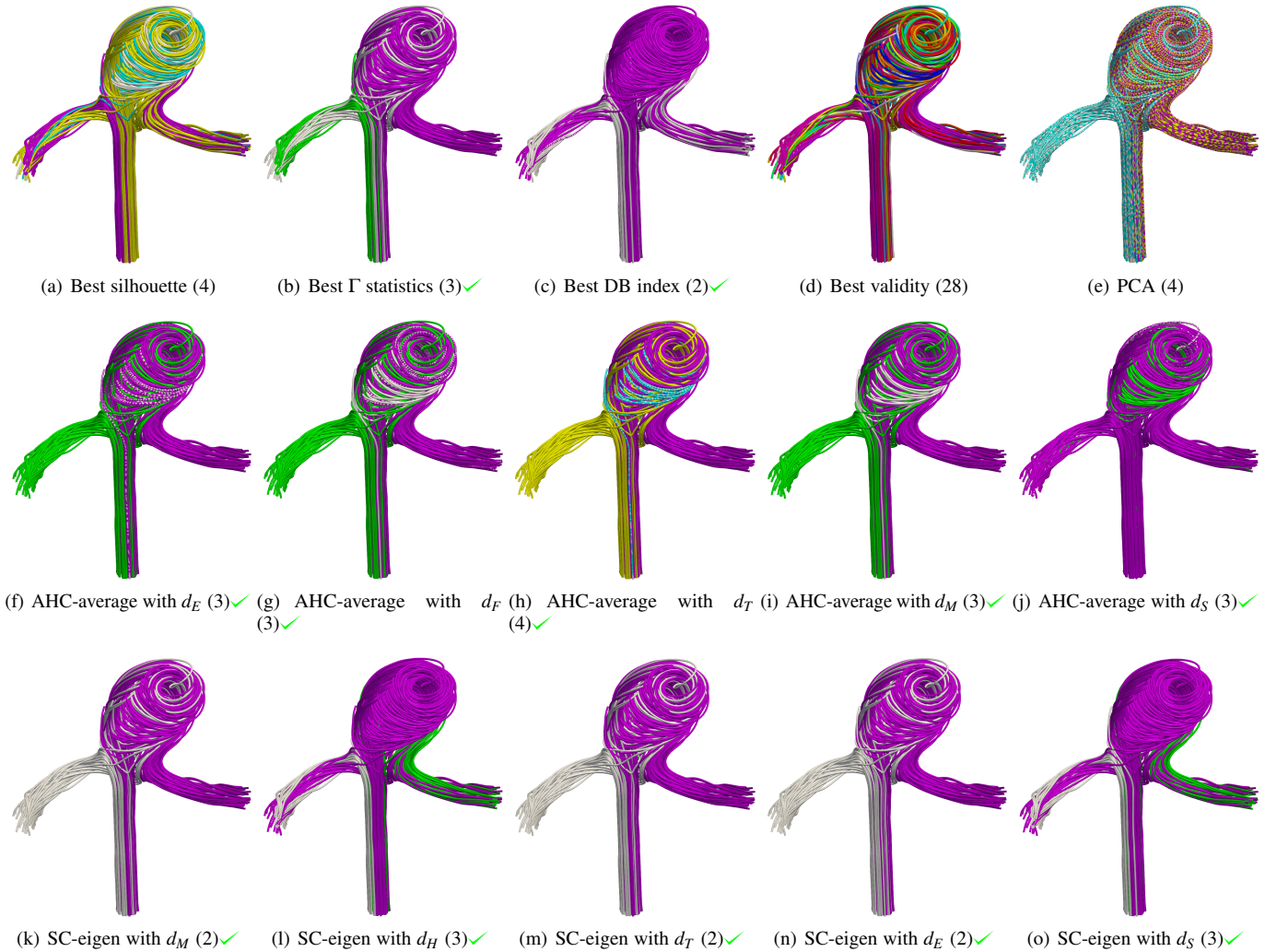


Fig. 14. Blood flow segmentation results of clustering (numbers of clusters are shown in the individual parentheses) according to the best evaluation metrics highlighted as blue in Fig.4 (see (a-d)), best average ranking-score clustering with highest ranking-score similarity measures (see (e-g)), and visually well-segmented combinations (see (h-j)), respectively. The visually good segmentation is marked as ✓.

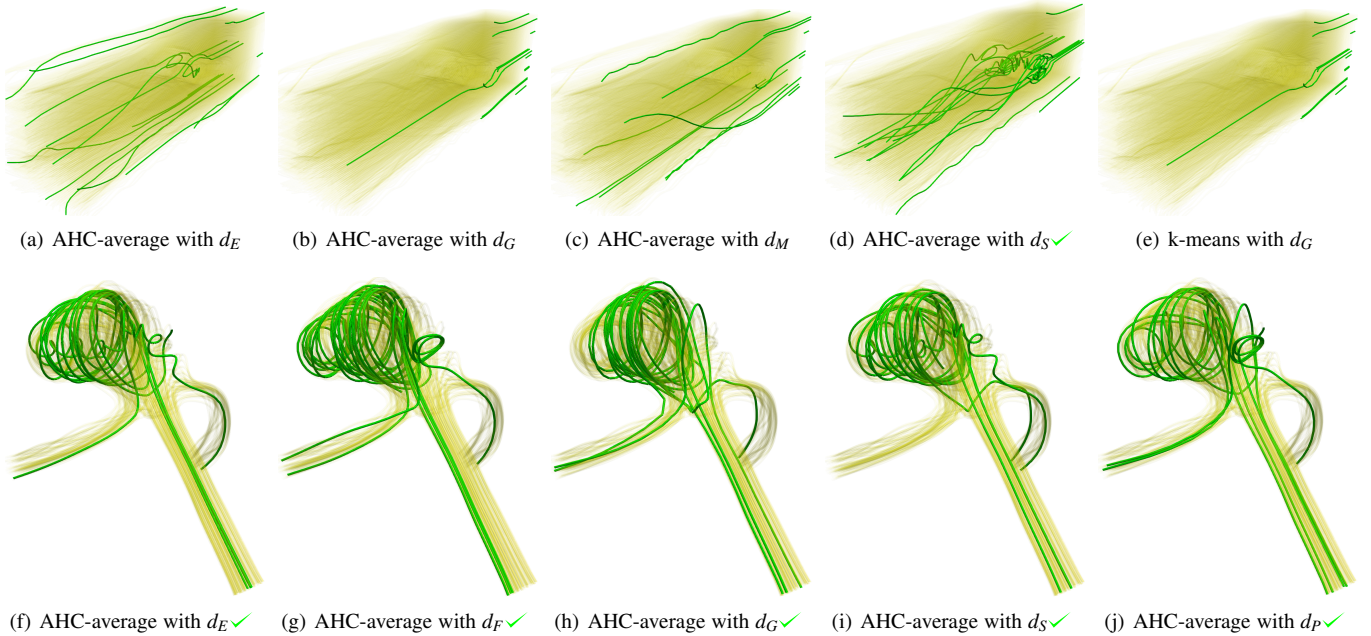


Fig. 15. Cylinder pathline (top row) and blood flow (bottom row) abstraction results of clustering with good abstraction marked as \checkmark . From the figures we can see that since blood flow has very clear structures, any similarity measure (either *spatial* or *shape-based*) can be used to extract the pathlines in vortex regions for abstraction. However, for complicated cylinder pathlines, only AHC-average with d_S can extract the pathlines rotating around the centroid cylinder while others cannot.